

## EXPLORING THE “ $L$ - $\sigma$ ” RELATION OF HII GALAXIES AND GIANT EXTRAGALACTIC HII REGIONS ACTING AS STANDARD CANDLES

YAN WU<sup>1</sup>, SHUO CAO<sup>1\*</sup>, JIA ZHANG<sup>2</sup>, TONGHUA LIU<sup>1†</sup>, YUTING LIU<sup>1</sup>, SHUAIBO GENG<sup>1</sup>, YUJIE LIAN<sup>1</sup>

*Draft version November 26, 2019*

### ABSTRACT

Cosmological applications of HII galaxies (HIIGx) and giant extragalactic HII regions (GEHR) to construct the Hubble diagram at higher redshifts require knowledge of the “ $L$ - $\sigma$ ” relation of the standard candles used. In this paper, we study the properties of a large sample of 156 sources (25 high- $z$  HII galaxies, 107 local HII galaxies, and 24 giant extragalactic HII regions) compiled by Terlevich et al. (2015). Using the cosmological distances reconstructed through two new cosmology-independent methods, we investigate the correlation between the  $H\beta$  emission-line luminosity  $L$  and ionized-gas velocity dispersion  $\sigma$ . The method is based on non-parametric reconstruction using the measurements of Hubble parameters from cosmic clocks, as well as the simulated data of gravitational waves from the third-generation gravitational wave detector (the Einstein Telescope, ET), which can be considered as standard sirens. Assuming the emission-line luminosity versus ionized gas velocity dispersion relation,  $\log L(H\beta) = \alpha \log \sigma(H\beta) + \kappa$ , we find the full sample provides a tight constraint on the correlation parameters. However, similar analysis done on three different sub-samples seems to support the scheme of treating HII galaxies and giant extragalactic HII regions with distinct strategies. Using the corrected “ $L$ - $\sigma$ ” relation for the HII observational sample beyond the current reach of Type Ia supernovae, we obtain a value of the matter density parameter,  $\Omega_m = 0.314 \pm 0.054$  (calibrated with standard clocks) and  $\Omega_m = 0.311 \pm 0.049$  (calibrated with standard sirens), in the spatially flat  $\Lambda$ CDM cosmology.

*Keywords:* HII regions — galaxies: general — cosmological parameters — cosmology: observations

### 1. INTRODUCTION

The Hubble diagram, which is directly related to the luminosity distances, has provided a useful method to probe cosmological parameters (Riess et al. 1998; Perlmutter et al. 1999). In order to measure the luminosity distance, we always turn to luminous sources of known (or standardizable) intrinsic luminosity in the Universe, such as type Ia supernova (SN Ia) (Cao, Liang & Zhu 2011; Cao & Liang 2013; Cao et al. 2015a; Chen et al. 2015; Qi et al. 2018) and less accurate but more luminous gamma-ray bursts (GRB) (Pan et al. 2015) in the role of “standard candles”. Powerful HII galaxies and extragalactic HII regions constitute a population that can be observed up to very high redshifts, reaching beyond feasible limits of supernova studies. Indeed, the power of modern cosmology lies in building up consistency rather than in single and precise experiments (Biesiada et al. 2010; Cao et al. 2015b; Ma et al. 2019), which indicates that every alternative method of restricting cosmological parameters is desired. It is known that HII galaxies and HII regions of galaxies could have very similar physical systems (Melnick et al. 1987; Wei et al. 2016), an outstanding feature of which lies in the rapidly forming stars surrounded by ionized hydrogen. More specifically, HII galaxies and HII regions may exhibit indistinguishable optical spectra, i.e., strong Balmer emission lines in  $H\alpha$  and  $H\beta$  due to the hydrogen ionized by the young mas-

sive star clusters (Searle & Sargent 1972; Bergeron 1977; Terlevich & Melnick 1981; Kunth & Östlin 2000).

A well-defined sample of HII galaxies with accurately measured flux density and the turbulent velocity of the gas could be useful to test cosmological parameters such as the present-day matter density, cosmic equation of state, etc. (Siegel et al. 2005; Plionis et al. 2011). Concerning such cosmological applications, the first method used for this purpose is of statistical nature. Essentially, the idea is to discuss an important phenomenon that as the mass of the starburst component increases, both the number of ionized photons and the turbulent velocity of the gas will increase. Therefore, one may naturally expect an quantitative relation between the luminosity  $L(H\beta)$  in  $H\beta$  and the ionized gas velocity dispersion  $\sigma$ , which has triggered numerous efforts to use HII galaxies for this purpose (Terlevich & Melnick 1981; Chávez et al. 2014). The first attempt to determine a possible correlation between the luminosity  $L(H\beta)$  and profile width for giant HII regions was presented in Melnick (1979), which was then extended to the luminosity-velocity dispersion relation satisfied by elliptical galaxies, bulges of spiral galaxies and globular clusters (Terlevich & Melnick 1981). It was found that in subsequent analysis (Melnick et al. 1987, 1988) that such “ $L$ - $\sigma$ ” relation, with small scattering can be used to determine cosmic distances independently of redshifts. More promising candidates in this context are HII galaxies (HIIGx) and giant extragalactic HII regions (GEHR) that can be observed up to very high redshifts. Following the suggestion proposed by Pettini et al. (1988), many authors furthermore confirmed the validity of the “ $L$ - $\sigma$ ” correlation at higher redshifts (Melnick et al. 2000),

<sup>1</sup>Department of Astronomy, Beijing Normal University, 100875, Beijing, China; caoshuo@bnu.edu.cn; liu-tonghua@mail.bnu.edu.cn

<sup>2</sup>School of physics and Electrical Engineering, Weinan Normal University, Shanxi 714099, China

which showed that HIIGx and GEHR can be used as independent distance indicators at  $z \sim 3$ .

From the original “ $L$ - $\sigma$ ” calibration of a sample of 5 high- $z$  HII galaxies covering the redshift range of  $2.1 < z < 3.4$  (Melnick et al. 1988), in combination with the measurements of flux density and turbulent gas velocity, Siegel et al. (2005) determined the best-fit value for the matter density parameter,  $\Omega_m = 0.21_{-0.12}^{+0.30}$  in the framework of flat  $\Lambda$ CDM model. A similar analysis was made by Plionis et al. (2011) concerning the so-called XCDM cosmology (with constant dark energy equation of state), using a revised zero-point of the original “ $L$ - $\sigma$ ” relation (Jarosik et al. 2011). While comparing the results from the previous “ $L$ - $\sigma$ ” relation, differences in central values of the best-fit cosmological parameters were also reported:  $\Omega_m = 0.22_{-0.04}^{+0.06}$ . The possible cosmological application of these HIIGx and GEHR as a standard candle has been extensively discussed in the literature (Fuentes et al. 2000; Bosch et al. 2002; Telles 2003; Siegel et al. 2005; Bordalo & Telles 2011; Plionis et al. 2011; Mania & Ratra 2012; Chávez et al. 2012, 2014; Wei et al. 2016), which found that the HII galaxies provides a competitive source of luminosity distance to probe the acceleration of the Universe. For instance, more recently, on a new sample of 156 sources compiled by Terlevich et al. (2015), Wei et al. (2016) have studied the possibility of utilizing HIIGx to carry out comparative studies between competing cosmologies, such as  $\Lambda$ CDM and the  $Rh = ct$  Universe (Melia 2007, 2013). However, it should be noted that cosmological application of the HIIGx and GEHR data requires good knowledge of the “ $L$ - $\sigma$ ” relation of the “standard candles” used. One of the major uncertainties was the typical value of the model parameters ( $\alpha$ ,  $\kappa$ ) of the emission-line luminosity versus ionized gas velocity dispersion relation,  $\log L(\text{H}\beta) = \alpha \log \sigma(\text{H}\beta) + \kappa$ . In order to obtain cosmological constraints, some authors chose to take  $\alpha$  and  $\kappa$  as statistical nuisance parameters (Wei et al. 2016). One should remember that the nuisance parameters characterizing the “ $L$ - $\sigma$ ” relation introduce considerable uncertainty to the final determination of other cosmological parameters. Having this in mind, properties of the HIIGx and GEHR data should be readdressed with the biggest sample to date (156 combined sources, including 25 high- $z$  HIIGx, 107 local HIIGx, and 24 GEHR) and taking into account reliable cosmological distance information based on current precise observations.

This encourages us to improve and develop it further, based on the newly-compiled sample of Hubble parameter  $H(z)$  measurements (which represents a type of new cosmological standard clock) and the simulated data of gravitational waves from the third-generation gravitational wave detector (which can be considered as standard siren). Compared with the previous works (Siegel et al. 2005; Plionis et al. 2011; Wei et al. 2016), the advantage of this work is that, we achieve a reasonable and compelling constraints on the “ $L$ - $\sigma$ ” relation in both the electromagnetic (EM) and gravitational wave (GW) window, using luminosity distances covering the HII redshift range derived in two cosmological-model-independent methods. This paper is organized as follows. We briefly introduce our methodology and the corresponding observational data (HII,  $H(z)$  and GW) in

Section II. Cosmological-model-independent constraints on the full sample and several sub-samples are presented in Section III. The cosmological application of the calibrated “ $L$ - $\sigma$ ” relation of HII regions are Section IV. Finally, the conclusions and discussions are presented in Section IV.

## 2. OBSERVATIONS

It is only quite recently when reasonable catalogues of HII galaxies and extragalactic HII regions containing more than 100 sources, with spectroscopic as well as astrometric data are becoming available. In this work, we have considered the current observations for 156 HII objects compiled by Terlevich et al. (2015). This data set was a larger sample of sources than used by Siegel et al. (2005) or by Plionis et al. (2011) and with more complete high-redshift data than used by Melnick et al. (1988).

On the one hand, the first complete sample from low-redshift ( $0.01 < z < 0.2$ ) HII galaxies selected from the SDSS DR7 spectroscopic catalogue is provided in (Abazajian 2009). It consists of 128 local HII galaxies satisfying the following well-defined selection criteria: 1) The lower limit of the equivalent widths of strongest emission lines relative to the continuum is  $\text{EW}(\text{H}\beta) > 50\text{\AA}$ , in order to guarantee the dominating contribution of a single young starburst to the total luminosity, without the contamination of underlying older population and older clusters (Dottori 1981; Dottori & Bica 1981; Melnick et al. 2000; Chávez et al. 2014; Wei et al. 2016)); 2) Extra objects with highly asymmetric emission lines should not be included in the final sample (Chávez et al. 2014); 3) The upper limit of the velocity dispersion is imposed as  $\log \sigma(\text{H}\beta) < 1.8$  km/s, in order to exclude rotationally supported systems and/or objects with multiple young ionizing clusters contributing to the total flux and affecting the line profiles (Chávez et al. 2014). When applying the former two criteria to the full sample, 14 objects are removed with the two cuts, while 7 more objects are excluded due to their high velocity dispersion measurements. Therefore, we have the “benchmark” catalog comprised of 107 local objects. On the other hand, we also use a combined sample of 25 high- $z$  HII galaxies covering the redshift range of  $0.64 \leq z \leq 2.33$  (taken from the XShooter spectrograph at the Cassegrain focus of the ESO-VLT (Terlevich et al. 2015) and the literature (Erb et al. 2006a,b; Masters et al. 2014)), as well as 24 giant HII regions in nine nearby galaxies (taken from Chávez et al. (2012)), which satisfy the well-defined observational selection criteria listed above. See Melnick et al. (1987) for the measured velocity dispersions and global integrated  $\text{H}\beta$  fluxes with corresponding extinction.

Full information about all 156 sources that remain after the aforementioned selection can be found in Table 1 of Wei et al. (2016), including source names, redshifts, categories, integrated  $\text{H}\beta$  flux, and corrected velocity dispersion. We remark here that, the final sample covers the redshift range  $0 < z < 2.33$ , which indicates its potential usefulness in cosmology at high redshifts. From observational perspective, the reddening corrected  $\text{H}\beta$  flux is measured by fitting a single Gaussian to the long-slit spectra (Terlevich et al. 2015), with the reddening corrections derived from the published  $E(B - V)$  using a

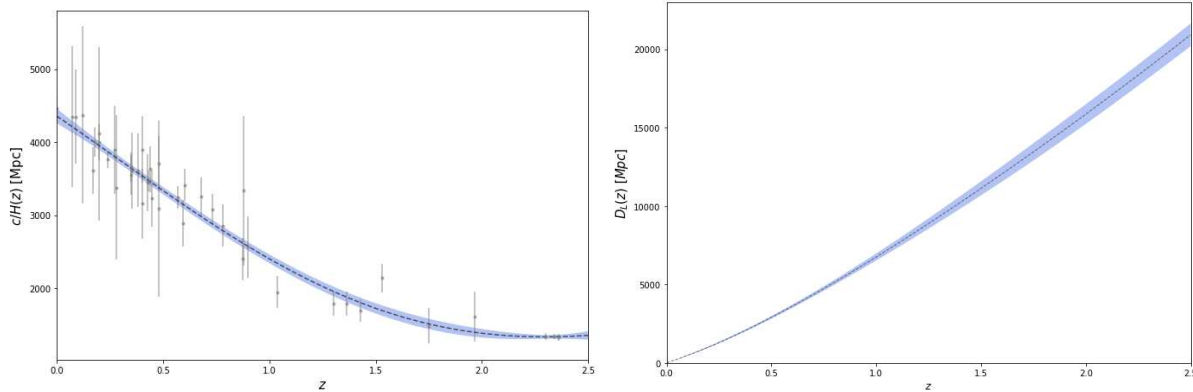


**Figure 1.** Left panel: Recent measurements of Hubble parameter measurements (black points) and the reconstruction of  $c/H(z)$  function with the GP; Right panel: The corresponding reconstructed luminosity distance  $D_L(z)$  with the GP (given the covariance matrix between the reconstructed  $c/H(z)$  points). The blue region represents the  $1\sigma$  confidence region.

standard reddening curve (Calzetti et al. 2000). The velocity dispersion inside the aperture can also be derived from the spectroscopic data. More specifically, one could obtain the velocity dispersion ( $\sigma_0$ ) and the corresponding  $1\sigma$  uncertainty from the full width at half-maximum (FWHM) measurement of the  $H\beta$  and  $[\text{OIII}]\lambda 5007$  line, i.e.,

$$\sigma_0 \equiv \frac{FWHM}{2\sqrt{2 \ln(2)}}. \quad (1)$$

Following the strategy of Wei et al. (2016), the final corrected velocity dispersion is defined as

$$\sigma = \sqrt{\sigma_0^2 - \sigma_{th}^2 - \sigma_i^2 - \sigma_{fs}^2}, \quad (2)$$

with the thermal broadening ( $\sigma_{th}$ ), instrumental broadening ( $\sigma_i$ ), and fine-structure broadening ( $\sigma_{fs}$ ). See Chávez et al. (2014) for more detailed discussion of the thermal and instrumental broadening, while the fine-structure broadening is taken as  $\sigma_{fs} = 2.4$  km/s, following the suggestion provided in García-Díaz et al. (2008).

The test of the “ $L$ - $\sigma$ ” relation of the standard candles requires a statistically complete and well-characterized (homogeneous) sample. Following the previous procedure applied to compact radio sources (Cao et al. 2015c, 2017a,b) and galactic-scale strong lensing systems (Cao et al. 2016), because our list includes a wide class of HII objects at different redshift, besides the full combined sample we will also consider separately three sub-samples: high- $z$  HIIGx, local HIIGx, and GEHR.

### 3. METHODOLOGY

Following the phenomenological model first proposed in Chávez et al. (2012) and later discussed in Chávez et al. (2014); Terlevich et al. (2015), the emission-line luminosity of a source is related to its ionized gas velocity dispersion as

$$\log L(H\beta) = \alpha \log \sigma(H\beta) + \kappa, \quad (3)$$

where  $\alpha$  is the constant slope parameter and  $\kappa$  represents the logarithmic luminosity at  $\log \sigma(H\beta) = 0$ . This is an empirical formula, whose scatter has been proved to be very small that it can be effectively used as a luminosity indicator in cosmology (Chávez et al. 2012; Terlevich et al. 2015). Meanwhile, The  $H\beta$  luminosity of

the sources is estimated from their reddening corrected flux density, which, assuming isotropic emission, reads

$$L(H\beta) = 4\pi D_L^2(z) F(H\beta), \quad (4)$$

where  $F(H\beta)$  is the reddening corrected  $H\beta$  flux and  $D_L(z)$  is the luminosity distance at redshift  $z$ .

The combination of Eq. (3)-(4) imply that if we could have a reliable knowledge of cosmological distances at different redshifts, then we would get stringent constraints on the range of parameters  $\alpha$  and  $\kappa$  describing HII sources. Compared with the previous procedure of simultaneously restricting  $(\alpha, \kappa)$  with the cosmological parameter  $\Omega_m$  (in the framework of  $\Lambda$ CDM, XCDM and  $Rh = ct$  cosmology) (Wei et al. 2016), in this work we try to place stringent constraints on the “ $L$ - $\sigma$ ” relation in both the electromagnetic (EM) and gravitational wave (GW) window, using luminosity distances covering the HII redshift range derived in two cosmological model-independent methods. Note that the strong degeneracies between  $\Omega_m$  and the two parameters characterizing the “ $L$ - $\sigma$ ” relation, not only confirm that the cosmological parameters are not independent of the nuisance parameters, but also attest to the motivation of our calculation (Wei et al. 2016).

In order to set limits on  $\alpha$  and  $\kappa$ , we turn to two catalogues of  $D_L(z)$  separately by two different methods. In the EM window, we will use luminosity distances derived in a cosmological model-independent way from  $H(z)$  measurements using Gaussian processes (GP) (Seikel et al. 2012a). As is well known, assuming the FLRW metric of a flat universe, the angular diameter distance can be written as

$$D_L(z) = (1+z) \int_0^z \frac{c dz}{H(z)}, \quad (5)$$

where  $c$  is the speed of light and  $H(z)$  is the Hubble parameter at redshift  $z$ . The idea of cosmological application of GP technique in general and with respect to  $H(z)$  data can be traced back to the paper of Holsclaw et al. (2010) and then extensively applied in more recent papers to test the cosmological parameters (Cao et al. 2017a, 2018), spatial curvature of the Universe (Cao et al. 2019; Qi et al. 2019a), and the speed of light at higher redshifts (Cao et al. 2017b). In this analysis, following the recent works of Zheng et al. (2019)

inspired by Gaussian processes (GPs), we have reconstructed the  $c/H(z)$  function from the recent Hubble parameter measurements including 41 data points from the galaxy differential age method and 10 data points from the radial BAO size method, and then derived  $D_L(z)$  covering the redshift range of HII observations<sup>3</sup>. See Qi et al. (2018); Zheng et al. (2019) for details and reference to the source papers. The advantage of the Gaussian processes is, we do not need to assume any parametrized model for  $H(z)$  while reconstructing this function from the data, which may provide more precise measurements of angular diameter distances at a certain redshift. We use the publicly available code called the GaPP (Gaussian Processes in Python)<sup>4</sup> to reconstruct the profile of  $H(z)$  function up to the redshifts  $z = 2.5$ , which can subsequently be used to reconstruct the luminosity distance.

The GP method uses some attributes of a Gaussian distribution, i.e., the reconstructed function  $f(z)$  follows a Gaussian distribution with a mean value  $\mu(z)$  and Gaussian error  $\sigma(z)$  at each point  $z$ . In this process, the values of the reconstructed function evaluated at any two different points ( $z$  and  $\tilde{z}$ ) are connected by a covariance function  $k(z, \tilde{z})$ , which depends only on a set of hyperparameters ( $\ell$  and  $\sigma_f$ ). Compared with the squared exponential covariance function widely used in the previous studies (Seikel et al. 2012a,b; Cai & Yang 2016; Yang et al. 2015; Qi et al. 2019a), we take the Matérn ( $\nu = 9/2$ ) form for the co-variance function

$$k(z, \tilde{z}) = \sigma_f^2 \exp\left(-\frac{3|z - \tilde{z}|}{\ell}\right) \times \left[1 + \frac{3|z - \tilde{z}|}{\ell} + \frac{27(z - \tilde{z})^2}{7\ell^2} + \frac{18|z - \tilde{z}|^3}{7\ell^3} + \frac{27(z - \tilde{z})^4}{35\ell^4}\right]. \quad (6)$$

where  $\sigma_f$  defines the overall amplitude of the correlation, and  $\ell$  gives a measure of the coherence length of the correlation. The reliability of the reconstructed function can be guaranteed by the fact that the hyper-parameters will be optimized by the GP with the observational data sets, which furthermore indicates that the reconstructed function is independent of the initial hyper-parameter settings. In this analysis, an issue which needs clarification is the achievable estimation of the  $1\sigma$  confidence region for the reconstructed function  $c/H(z)$ . Note that the  $1\sigma$  confidence region depends on both the actual errors of individual data points ( $\sigma_{\frac{c}{H(z)}}$ ) and the product  $K_* K^{-1} K_*^T$ . Here  $K_*$  is the covariance matrix at redshift  $z_*$ , which is calculated from the original  $c/H(z)$  data at  $z_i$  and the covariance matrix  $k$ :

$$K_* = [k(z_1, z_*), k(z_2, z_*), \dots, k(z_i, z_*)]. \quad (7)$$

It should be pointed out that, when there is a large correlation between the data ( $K_* K^{-1} K_*^T > \sigma_f$ ), the dispersion at point  $z_i$  will be less than  $\sigma_{\frac{c}{H(z)}}$  and the reconstructed  $1\sigma$  regions will correspondingly become smaller.

More specifically, it was shown in the previous analysis (Seikel et al. 2012a,b) that the correlation between any two points  $z$  and  $\tilde{z}$  will be large only when  $z - \tilde{z} < \sqrt{2}\ell$ , which is clearly satisfied by the current  $H(z)$  data used in our analysis. Therefore, as can be seen from the reconstructed results shown in Fig. 1, the GP estimated  $1\sigma$  confidence region is much smaller than the uncertainties in the original  $c/H(z)$  data. Such issue has been extensively discussed in Seikel et al. (2012a). Using the reconstructed profile of  $c/H(z)$  function up to the redshifts  $z \sim 2.5$ , we are able to reconstruct the luminosity distance  $D_L(z)$  with the aforementioned Gaussian processes. One should note that the error band should be interpreted in a redshift by redshift sense and the covariances are not visible in such a plot (Seikel et al. 2012a). Following the commonly-used procedure transforming  $c/H(z)$  data into luminosity distance (Holanda et al. 2012), the  $D_L(z)$  function can be calculated by a usual simple trapezoidal rule (through Eq. (5)). With the standard error propagation formula, the error associated to the  $i$ th redshift bin is given by  $s_i = \frac{1}{2} \left( \sigma_{\frac{c}{H(z_i)}}^2 + \sigma_{\frac{c}{H(z_{i+1})}}^2 \right)$ , where  $\sigma_{\frac{c}{H(z)}}$  is the error of the  $c/H(z)$  data reconstructed from Gaussian processes. However, it should be noted that the constructed luminosity distances are correlated, since all of the derived  $s_i$  are statistically dependent on each other (Liao et al. 2017). More specifically, the  $c/H(z)$  data are Gaussian Process reconstructed, following a multidimensional Gaussian distribution with the covariance matrix (through Eq. (7)). Hence, the uncertainty of the luminosity distance corresponding to certain redshift  $z$  should include statistical uncertainties and the covariances between every  $c/H(z)$  pair among the total data. That is,

$$\sigma_{D_{L,H(z)}}^2 = \frac{(\Delta z)^2}{2} \left[ \sum_{i=1}^n s_i + \sum_{i=2}^n \sum_{j=1}^{i-1} \text{Cov} \left( \frac{c}{H(z_i)}, \frac{c}{H(z_j)} \right) \right], \quad (8)$$

where  $\Delta z$  is the length of the redshift bin, while Cov denotes the covariance matrix for a set of reconstructed  $c/H(z)$  points given by Eq. (7). The results are also shown in Fig. 1, where the reconstructed  $D_{L,H(z)}$  function with corresponding  $1\sigma$  uncertainty strip are displayed. Distance reconstruction with the Hubble parameter measurements is denoted as ‘‘Cosmology-independent method I’’.

In the GW window, we turn to the simulated data of gravitational waves from the third-generation gravitational wave detector, which can be considered as standard siren to provide the information of luminosity distance. Gravitational waves provide us with a completely new means of observation and are also a promising probe for cosmology. It is well known that the detection of gravitational waves (GW) from the merger of double compact object (DCO) (Abbott et al. 2016, 2017) has opened the new era of GW astronomy. The original idea of using the waveform signal to directly measure the luminosity distance  $D_L$  to the GW sources can be traced back to the paper of Schutz (1986), which indicates the inspiraling and merging compact binaries consisting of neutron stars (NSs) and black holes (BHs), can be used to constrain the Hubble constant by combining

<sup>3</sup> The Hubble constant  $H_0 = 67.3$  km/s/Mpc from the latest Planck CMB observations (Planck Collaboration 2018) is also taken for distance reconstruction in our analysis.

<sup>4</sup> <http://www.acg.uct.ac.za/~seikel/GAPP/index.html>

**Table 1**

Summary of the constraints on the “ $L$ - $\sigma$ ” relation parameters obtained with the full sample and three sub-samples (see text for definitions).

Sample (Calibration method+Cosmology)	$\alpha$	$\kappa$
Full sample (Cosmology-independent method I)	$\alpha = 5.10 \pm 0.10$	$\kappa = 33.12 \pm 0.15$
Full sample (Cosmology-independent method II+Planck)	$\alpha = 5.13 \pm 0.08$	$\kappa = 33.06 \pm 0.13$
Full sample (Cosmology-independent method II+WAMP9)	$\alpha = 5.17 \pm 0.09$	$\kappa = 32.86 \pm 0.12$
High- $z$ HIIGx (Cosmology-independent method I)	$\alpha = 5.18 \pm 0.65$	$\kappa = 33.00 \pm 1.13$
Local HIIGx (Cosmology-independent method I)	$\alpha = 4.88 \pm 0.15$	$\kappa = 33.48 \pm 0.22$
GEHR (Cosmology-independent method I)	$\alpha = 5.77 \pm 0.52$	$\kappa = 32.25 \pm 0.62$
High- $z$ HIIGx (Cosmology-independent method II)	$\alpha = 5.33 \pm 0.65$	$\kappa = 32.70 \pm 1.13$
Local HIIGx (Cosmology-independent method II)	$\alpha = 4.93 \pm 0.14$	$\kappa = 33.39 \pm 0.22$
GEHR (Cosmology-independent method II)	$\alpha = 5.81 \pm 0.50$	$\kappa = 32.19 \pm 0.61$

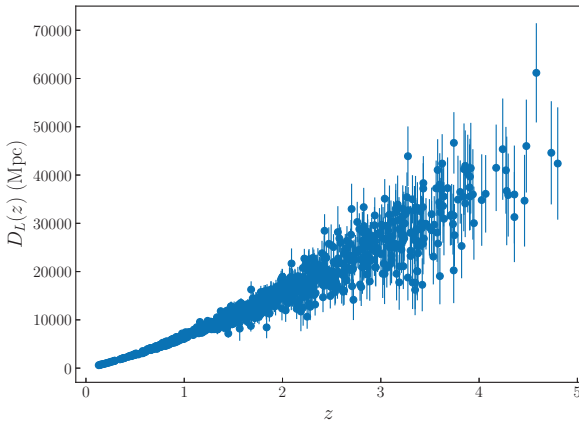


**Figure 2.** The luminosity distance measurements from 1000 GW events detected by ET.

the redshift information of source. Therefore, gravitational wave signals from the merger of DCOs are put forward as distance indicators and are called standard sirens (Dalal et al. 2006; Taylor, et al. 2012; Zhao et al. 2011; Cai et al. 2015; Cai & Yang 2017). If we can locate the host galaxy by means of EM counterparts, redshift information of the GW source can be easily obtained. In this paper we simulate GW events based on the Einstein Telescope, the third generation of the ground-based GW detector (The Einstein Telescope Project 2015). Although only a few GW events have been detected by the current advanced ground-based detectors (i.e., the advanced LIGO and Virgo detectors), ET will expand the detection space by three orders of magnitude, and thus can detect much more GW events (Cai et al. 2015; Cai & Yang 2017). In this paper, we carry out a Monte Carlo simulation of the GW signals of NS-NS and NS-BH systems with high signal to noise ratio (SNR), based on future observations from the third generation technology (the “xylophone” configuration) (Cai et al. 2015). The specific steps to simulate the mock data is similar with that used in Qi et al. (2019b,c). Concerning the error strategy, the combined signal-to-noise ratio (SNR) for the network not only helps us confirm the detection of GW with  $\rho_{net} > 8$ , the SNR threshold currently used by LIGO/Virgo network, but also contribute to the error on the luminosity distance as  $\sigma_{D_{L,GW}}^{inst} \simeq \frac{2D_{L,GW}}{\rho}$  (Zhao et al. 2011). Mean-

while, the lensing uncertainty caused by the weak lensing is also taken into consideration, which is modeled as  $\sigma_{D_{L,GW}}^{lens}/D_{L,GW} = 0.05z$  (Sathyaprakash et al. 2010; Li 2015). Therefore, the distance precision per GW is taken as

$$\begin{aligned} \sigma_{D_{L,GW}} &= \sqrt{(\sigma_{D_{L,GW}}^{inst})^2 + (\sigma_{D_{L,GW}}^{lens})^2} \\ &= \sqrt{\left(\frac{2D_{L,GW}}{\rho}\right)^2 + (0.05zD_{L,GW})^2}. \end{aligned} \quad (9)$$

In this paper, we take the flat  $\Lambda$ CDM universe as our fiducial model in the simulation. The matter density parameter  $\Omega_m = 0.315$  and the Hubble constant  $H_0 = 67.3$  km/s/Mpc from the latest Planck CMB observations (Planck Collaboration 2018) is taken for Monte Carlo simulations in our analysis. Following the redshift distribution of GW sources taken as (Sathyaprakash et al. 2010) and assuming the luminosity distance measurements obey the Gaussian distribution, the simulated 1000 GW events used for statistical analysis in the next section are shown in Fig. 2. In our analysis, in order to get  $D_L$  at the redshift of HII galaxy, we have employed the Gaussian Processes (GPs) to reconstruct the function  $D_{L,GW}(z)$  and its corresponding  $1\sigma$  uncertainty  $\sigma_{D_{L,GW}}$ . Distance reconstruction with the simulated GW sample is denoted as “Cosmology-independent method II”.

Now, from the observational point of view, in the framework of “ $L$ - $\sigma$ ” relation, the observed distance modulus of an HII object is

$$\mu_{obs} = 2.5[\kappa + \alpha \log \sigma(\text{H}\beta) - \log F(\text{H}\beta)] - 100.2, \quad (10)$$

with the corresponding error  $\sigma_{\mu_{obs}}$  expressed as  $\sigma_{\mu_{obs}} = \sqrt{(2.5\alpha\sigma_{\log\sigma})^2 + (2.5\sigma_{\log F})^2}$ . Here  $\sigma_{\log\sigma}$  and  $\sigma_{\log F}$  represent the standard errors of the reddening corrected H $\beta$  flux ( $\log \sigma(\text{H}\beta)$ ) and the corrected velocity dispersion ( $\log F(\text{H}\beta)$ ). For each HII galaxy, the reconstructed distance modulus  $\mu_{th}$  can be calculated from the measured redshift  $z$  by the definition

$$\mu_{th} \equiv 5 \log \left[ \frac{D_L(z)}{\text{Mpc}} \right] + 25, \quad (11)$$

where  $D_L(z)$  is the cosmology-dependent luminosity distance obtained through “Cosmology-independent method I” and “Cosmology-independent method II”. The propagated uncertainty of  $\mu_{th}$  is given by  $\sigma_{\mu_{th}} =$

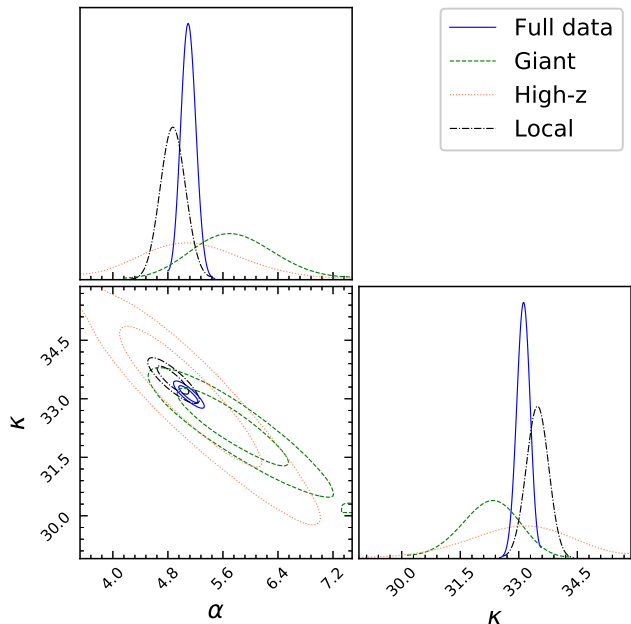


**Figure 3.** Constraints on HII parameters obtained from the full sample and three sub-samples (high- $z$  HIIGx, local HIIGx, and GEHR), based on the  $D_L(z)$  function reconstructed from current  $H(z)$  data (“Cosmology-independent method I”).

$\frac{5\sigma_{D_L}}{D_L \ln 10}$ . We determine the parameters ( $\alpha$  and  $\kappa$ ) characterizing HII objects by minimizing the  $\chi^2$  objective function

$$\chi^2(\alpha, \kappa) = \sum_i \frac{(\mu_{obs}(z_i; \alpha, \kappa) - \mu_{th}(z_i))^2}{\sigma_{\mu,i}^2} \quad (12)$$

and the corresponding statistical error is given by

$$\sigma^2 = (2.5\alpha\sigma_{\log \sigma})^2 + (2.5\sigma_{\log F})^2 + \left(\frac{5\sigma_{D_L}}{D_L \ln 10}\right)^2. \quad (13)$$

Note that the observational statistical uncertainty for the  $i$ th data point and the uncertainty for the reconstructed distance modulus are both included. Then using the Markov Chain Monte Carlo technique available within CosmoMC package (Lewis & Bridle 2002), we perform Monte Carlo simulations of the posterior likelihood  $\mathcal{L} \sim \exp(-\chi^2/2)$  and apply a public python package “triangle.py” from Foreman-Mackey et al. (2013) to plot our constraint contours.

#### 4. RESULTS AND DISCUSSIONS

In this section, we focus our attention on the constraints on the parameters ( $\alpha$  and  $\kappa$ ) obtained from different samples, i.e., the full  $N = 156$  sample, as well as three sub-samples determined from high- $z$  HIIGx, local HIIGx, and GEHR. The results are summarized in Table I. The graphic representations of the probability distribution of  $\alpha$  and  $\kappa$  are presented in Figs. 3-4, in which one can see the 1-D distributions for each parameter and  $1\sigma$ ,  $2\sigma$  contours for the joint distribution.

To start with, by applying the above mentioned  $\chi^2$ -minimization procedure to the distance reconstruction with the Hubble parameter measurements (“Cosmology-independent method I”), we obtain the results shown

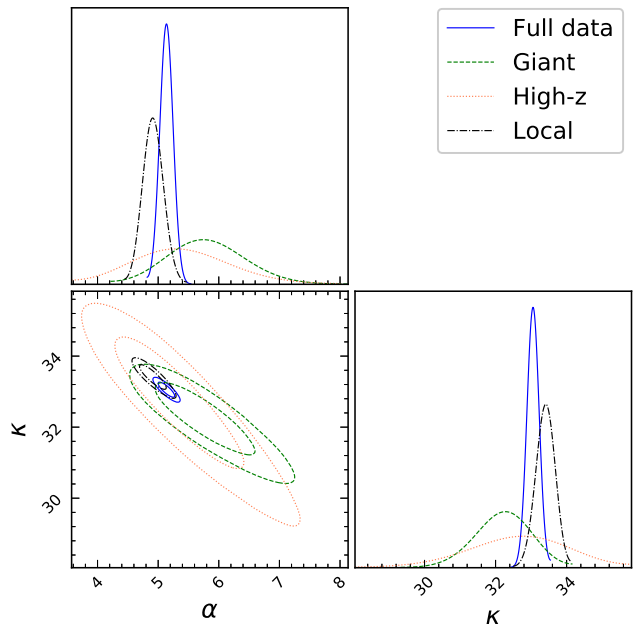


**Figure 4.** Constraints on HII parameters obtained from the full sample and three sub-samples (high- $z$  HIIGx, local HIIGx, and GEHR), based on the  $D_L(z)$  measurements from future simulated GW data (“Cosmology-independent method II”).

in Fig. 3. Performing fits on the full data comprising 156 objects, we obtain the following best-fit values and corresponding  $1\sigma$  uncertainties (68.3% confidence level):

$$\begin{aligned} \alpha &= 5.10 \pm 0.10, \\ \kappa &= 33.12 \pm 0.15. \end{aligned}$$

Marginalized  $1\sigma$  and  $2\sigma$  contours of each parameter obtained are shown in Fig. 3. It is obvious that, the full sample analysis has also yielded improved constraints on the meaningful physical parameters:  $\alpha$  and  $\kappa$ . More importantly, we find that our constraints on the two parameters with “Cosmology-independent method I” are very different from those obtained in the framework of different cosmologies. For instance, some researchers (Wei et al. 2016) have previously derived a fit to the flat  $\Lambda$ CDM, XCDM and  $Rh = ct$  cosmology, with the optimized parameter values for the  $\alpha$  parameter:  $\alpha = 4.89 \pm 0.09$ ,  $\alpha = 4.87 \pm 0.10$  and  $\alpha = 4.86 \pm 0.08$ , which disagrees with our results at 68.3% C. L. Therefore, the values of the two best-fit parameters of the phenomenological formula obtained in our analysis, if confirmed by future investigation of HII observations, will offer additional constraints for cosmological tests based on “ $L-\sigma$ ” relation of extragalactic sources.

In Table 1 and Fig. 3, we show the results of fitting the two parameters,  $\alpha$  and  $\kappa$ , on three sub-samples described in Section II. It is interesting to note that the ranges of  $\alpha$  and  $\kappa$  for local HII galaxies ( $\alpha = 4.88 \pm 0.15$ ,  $\kappa = 33.48 \pm 0.22$ ) are marginally close to estimates obtained from High- $z$  HII galaxies ( $\alpha = 5.18 \pm 0.65$ ,  $\kappa = 33.00 \pm 1.13$ ). On the other hand, the constrained results for giant extragalactic HII regions (GEHR), which constitute the most important part of our full HII sample are particularly interesting. Namely, one can clearly see that the best-fit values of the two parameters for this

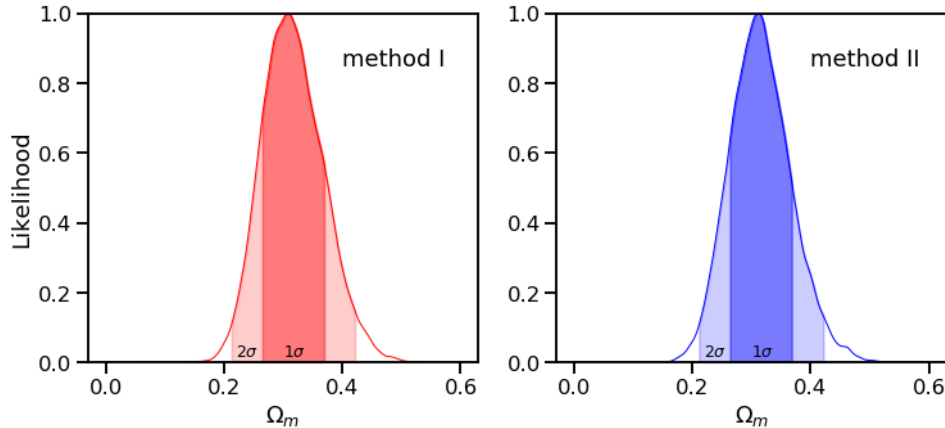


**Figure 5.** Cosmological fits on the flat  $\Lambda$ CDM model obtained from the full sample, based on the corrected “ $L$ - $\sigma$ ” relation with the current  $H(z)$  data (left panel) and future simulated GW data (right panel).

population,  $\alpha = 5.77 \pm 0.52$  and  $\kappa = 32.25 \pm 0.62$ , are significantly different from the corresponding quantities of HII galaxies. Substantial distinction between  $\alpha$  and  $\kappa$  parameters exists for the two sub-populations (GEHR and HIIGx) is more clear when the  $1\sigma$  uncertainties are taken into consideration. Consequently, our results indicate the different “ $L$ - $\sigma$ ” relation of HII regions acting as standard candles.

Then one issue which might be raised is the choice of the  $D_A(z)$  function reconstructed from current  $H(z)$  data in the course our estimation of  $\alpha$  and  $\kappa$ . Therefore, we have undertaken a similar analysis with the second model-independent approach, the simulated data of gravitational waves from the third-generation gravitational wave detector<sup>5</sup>. In this case, performing fits on the full data set, the 68.3% confidence level uncertainties on the three model parameters are:

$$\begin{aligned}\alpha &= 5.13 \pm 0.08, \\ \kappa &= 33.06 \pm 0.13.\end{aligned}$$

Fig. 4 shows these constraints in the parameter space of  $\alpha$  and  $\kappa$ . Comparing constraints based on the two model-independent methods, we see that confidence regions of  $\alpha$  and  $\kappa$  are well overlapped with each other; hence our results and discussions presented above are robust. This tendency could also be found in fits performed on three sub-samples with local HII galaxies, high- $z$  HII galaxies, and giant extragalactic HII regions. From the results displayed in Fig. 4, one can find the obtained value of  $\alpha$  and  $\kappa$  from our sub-sample with giant extragalactic HII regions, whose confidence contours in the  $(\alpha, \kappa)$  parameter plane differ from the other two remaining samples. More specifically, in the framework of the “ $L$ - $\sigma$ ” relation for giant extragalactic HII regions, a lower value of the slope parameter and a higher value of the logarithmic luminosity at  $\log \sigma(H\beta) = 0$  is revealed and supported by our analysis. We must keep in mind that similarity or difference in  $(\alpha, \kappa)$  parameters for HII observations with different types of optical counterparts might reveal similar or different physical processes governing the  $H\beta$

<sup>5</sup> Note that in the second approach with simulated GW data, we pay more attention to demonstrating the improvements that future GW measurements could provide, concerning the calibration of the “ $L$ - $\sigma$ ” relation.

emission in GEHR and HIIGx. To some extent, our results imply the need of treating these classes of HII observations separately in future cosmological studies.

The second issue which needs clarification is the fiducial cosmology used in our GW simulation, i.e., the consistency between the luminosity distance coming from GP reconstructed  $H(z)$  and the simulated GW standard siren should be fully tested. In order to explore the potential systematics caused by different priors of cosmological parameters, besides assuming a flat  $\Lambda$ CDM model with parameters coming from Planck 2018 observations, we also consider the WMAP nine year results (WMAP9) for comparison, in which the matter density parameter and the Hubble constant are respectively taken as  $\Omega_m = 0.279$  and  $H_0 = 70.0$  km/s/Mpc (Hinshaw et al. 2013). In this case, the full data set provides the best fit on the “ $L$ - $\sigma$ ” relation as

$$\begin{aligned}\alpha &= 5.17 \pm 0.09, \\ \kappa &= 32.86 \pm 0.12.\end{aligned}$$

Comparing constraints based on Planck and WMAP9 observations shown in Table 1, one could see that confidence regions of  $\alpha$  and  $\kappa$  are almost the same. We remark here that, considering that the WMAP9 and Planck data are consistent with the accuracy sufficient to the comparison with the “ $L$ - $\sigma$ ” relation, it is not surprising that the regression results of the “ $L$ - $\sigma$ ” relation in combination with WMAP and Planck are compatible in the framework of  $\Lambda$ CDM cosmology (Cao et al. 2015c).

Having performed cosmological-model-independent analysis, we can also investigate cosmological implications of the distance modulus of 156 HII measurements by taking the corrected “ $L$ - $\sigma$ ” relation into consideration. In this analysis we focus on the  $\Lambda$ CDM model when spatial flatness of the FLRW metric is assumed, which is strongly indicated by the location of the first acoustic peak in the CMBR (Planck Collaboration 2018) and also independently supported by the quasar data at  $z \sim 3.0$  as demonstrated in (Cao et al. 2019). The Friedmann equation is

$$H^2 = H_0^2 [\Omega_m(1+z)^3 + 1 - \Omega_m], \quad (14)$$

where  $\Omega_m$  parameterizes the density of matter (both baryonic and non-baryonic components) in the Universe.

For the flat  $\Lambda$ CDM model, different from the methods used in Wei et al. (2016), we examine the probability distributions of  $\Omega_m$  by considering the best-fitted  $\alpha$  and  $\beta$  parameters (with their  $1\sigma$  uncertainties) obtained from the previous model-independent tests. Fitting the  $\Lambda$ CDM model to the full sample with the corrected “ $L$ - $\sigma$ ” relation, one is able to get the observational constraint on the matter density parameter as  $\Omega_m = 0.314 \pm 0.054$  (calibrated with standard clocks in EM domain) and  $\Omega_m = 0.311 \pm 0.049$  (calibrated with standard sirens in GW domain). The results are shown in Fig. 5. On the one hand, one may observe that the results obtained from the combined HII sample are well consistent with the fit based on the full-mission Planck observations of temperature and polarization anisotropies of the CMB radiation (Planck Collaboration 2018), as well as a newly compiled data set of mas compact radio sources representing intermediate-luminosity quasars covering the redshift range  $0.5 < z < 2.8$  (Cao et al. 2017a,b; Li et al. 2017; Xu et al. 2018). On the other hand, our results strongly suggest that the dynamical properties of HII galaxies may significantly impact the likelihood distributions of  $\Omega_m$  and thus constraints on the properties of dark energy. This conclusion is strengthened by the comparison of our cosmological fits from the recalibrated “ $L$ - $\sigma$ ” relation through our cosmological-model-independent tests and those based on a specific cosmological scenario (Wei et al. 2016). Therefore, although the constraints resulting from this analysis are marginally consistent with the previous works, our results based on a cosmological-model-independent check (especially “Cosmology-independent method I”) could be useful as hints for priors on  $\alpha$  and  $\kappa$  parameters in future cosmological studies using HII observations.

## 5. CONCLUSION

In this paper, we explored the properties of a sample of 156 HII galaxies (HIIGx) and giant extragalactic HII regions (GEHR) with measured flux density and turbulent gas velocity. The “ $L$ - $\sigma$ ” relation of these standard candles is usually parameterized as  $\log L(\text{H}\beta) = \alpha \log \sigma(\text{H}\beta) + \kappa$ . Using the cosmological distances reconstructed through two new cosmology-independent methods, we investigate the correlation between the emission-line luminosity  $L$  and ionized-gas velocity dispersion  $\sigma$ . The method is based on non-parametric reconstruction using the measurements of Hubble parameters from cosmic clocks, as well as the simulated data of gravitational waves from the third-generation gravitational wave detector (the Einstein Telescope, ET), which can be considered as standard sirens. Moreover, we have also investigated cosmological implications of the distance modulus of 156 HII measurements by taking the corrected “ $L$ - $\sigma$ ” relation into consideration, which encourages us to probe cosmological parameters beyond the current reach of Type Ia supernovae. Here we summarize our main conclusions in more detail:

- In the full sample, we find that measurements of HIIGx and GEHR provide tighter estimates of the “ $L$ - $\sigma$ ” relation parameters. Performing fits on the full data comprising 156 objects, we obtain the following best-fit values and corresponding  $1\sigma$  uncertainties (68.3% confidence level):  $\alpha =$

$5.10 \pm 0.10$ ,  $\kappa = 33.12 \pm 0.15$  (calibrated with standard clocks in EM domain) and  $\alpha = 5.13 \pm 0.08$ ,  $\kappa = 33.06 \pm 0.13$  (calibrated with standard sirens in GW domain). We have also explored the potential systematics caused by different priors of cosmological parameters in GW simulation. In the framework of a flat  $\Lambda$ CDM model with parameters coming from WMAP9, the full data set provides the best fit on the “ $L$ - $\sigma$ ” relation:  $\alpha = 5.17 \pm 0.09$  and  $\kappa = 32.86 \pm 0.12$  (calibrated with standard sirens in GW domain). More importantly, our constraints on the two parameters with two new cosmology-independent methods are very different from those obtained in the framework of different cosmologies.

- Furthermore, we divide the full sample into three different sub-samples according to their optical counterparts. It turns out that the ranges of  $\alpha$  and  $\kappa$  for local HII galaxies are marginally close to estimates obtained from High- $z$  HII galaxies. The best-fit values for giant extragalactic HII regions (GEHR) are significantly different from the corresponding quantities of HII galaxies. Substantial distinction between  $\alpha$  and  $\kappa$  parameters exists for the two sub-populations (GEHR and HIIGx) is more clear when the  $1\sigma$  uncertainties are taken into consideration. Consequently, closeness or difference of parameter values for different types of counterparts indicate the similar or different “ $L$ - $\sigma$ ” relation of HII regions acting as standard candles, as well as the existence of possible similar or different physical processes governing the  $\text{H}\beta$  emission in GEHR and HIIGx.
- Fitting the  $\Lambda$ CDM model to the full sample with the corrected “ $L$ - $\sigma$ ” relation, one is able to get the observational constraint on the matter density parameter as  $\Omega_m = 0.314 \pm 0.054$  and  $\Omega_m = 0.311 \pm 0.049$ , which is inconsistent with the previous results obtained on the same sample but agrees very well with other recent astrophysical measurements including Planck observations. Therefore, it is strongly suggested that reliable knowledge of the dynamical properties of HII galaxies may significantly impact the constraints on relevant cosmological parameters. The values of the two best-fit parameters of the “ $L$ - $\sigma$ ” relation obtained in our analysis, if confirmed by future investigation of HII observations, will offer additional constraints for cosmological tests based on extragalactic sources.
- As a final remark, we point out that the sample discussed in this paper is based on HII objects discovered in different surveys. Our analysis potentially may suffer from systematics stemming from this inhomogeneity. Therefore, we may expect more vigorous and convincing constraints on the dynamical properties of HII galaxies within the coming years with more precise data, especially a larger sample of high- $z$  HIIGx observed by the current facilities such as the K-band Multi Object Spectrograph at the Very Large Telescope (Terlevich et al. 2015).

We are grateful to Jingzhao Qi for helpful discus-



sions. This work was supported by National Key R&D Program of China No. 2017YFA0402600, the National Natural Science Foundation of China under Grants Nos. 11503001, 11690023, 11373014, and 11633001, the Strategic Priority Research Program of the Chinese Academy of Sciences, Grant No. XDB23000000, the Interdiscipline Research Funds of Beijing Normal University, and the Opening Project of Key Laboratory of Computational Astrophysics, National Astronomical Observatories, Chinese Academy of Sciences.

## REFERENCES

- Abazajian, K.N. et al. 2009, *ApJS*, 182, 543  
 Abbott, B. P., et al. (LIGO Scientific and Virgo Collaborations), *PPL*, 116 061102 (2016).  
 Abbott, B., et al. (LIGO Scientific and Virgo Collaborations), 2017, *Nature*, 551, 85  
 Bergeron, J. 1977, *ApJ*, 211,62  
 Biesiada, M., et al. 2010, *MNRAS*, 406, 1055  
 Bordalo, V., Telles, E. 2011, *ApJ*, 735, 52  
 Bosch, G., Terlevich, E., Terlevich, R. 2002, *MNRAS*, 329, 481  
 Cai, R.-G., et al. arXiv:1509.06283  
 Cai, R., Guo, Z., & Yang, T., 2016, *PRD*, 93, 043517  
 Cai, R.-G. & Yang, T. 2017, *PRD*, 95, 044024  
 Cao, S., Liang N., & Zhu, Z.-H. 2011, *MNRAS*, 416, 1099  
 Cao, S. & Liang, N. 2013, *IJMPD*, 22, 1350082  
 Cao, S., et al. *IJTP*, 2015, 54, 1492  
 Cao, S., et al. 2015, *ApJ*, 806, 185  
 Cao, S., et al. 2015, *ApJ*, 806, 66  
 Cao, S., et al. 2016, *MNRAS*, 461, 2192  
 Cao, S., et al. 2017, *JCAP*, 02, 012  
 Cao, S., et al. 2017, *A&A*, 606, A15  
 Cao, S., et al. 2018, *EPJC*, 78, 749  
 Cao, S., et al. 2019, *PDU*, 24, 100274  
 Calzetti, D., et al. 2000, *ApJ*, 533, 682  
 Chávez, R., et al. 2012, *MNRAS*, 425, L56  
 Chávez, R., et al. 2014, *MNRAS*, 442, 3565  
 Chen, Y., et al. 2015, *JCAP*, 02, 010  
 Dalal, N., Holz, D. E., Hughes, S.A., Jain, B. 2006, *PRD*, 74, 063006  
 Dottori, H. A. 1981, *Ap&SS*, 80, 267  
 Dottori, H. A., Bica, E. L. D. 1981, *A&A*, 102, 245  
 Erb, D. K., et al. 2006a, *ApJ*, 647, 128  
 Erb, D. K., et al. 2006b, *ApJ*, 646, 107  
 Foreman-Mackey, D., et al. 2013, *PASP*, 125, 306  
 Fuentes-Masip, O., et al. 2000, *AJ*, 120, 752  
 García-Díaz, M. T., et al. 2008, *RMxAA*, 44, 181  
 Hinshaw G., et al., 2013, *ApJS*, 208, 19  
 Holanda, R. F. L., et al. 2012, arXiv: 1207.1694.  
 Holsclaw, T., et al. 2010, *PRL*, 105, 241302  
 Jarosik, N., et al. 2011, *ApJS*, 192, 14  
 Kunth, D., & Östlin, G. 2000, *A&ARv*, 10, 1  
 Lewis, A., & Bridle, S. 2002, *PRD*, 66, 103  
 Li, T. G., *Extracting Physics from Gravitational Waves: Testing the Strong-field Dynamics of General Relativity and Inferring the Large-scale Structure of the Universe*, 2015, Springer  
 Liao, K., et al. 2015, *PRD*, 92, 123539  
 Li, X. L., et al. 2017, *EPJC*, 77, 677  
 Ma, Y., et al. 2019, *EPJC*, 79, 121  
 Mania, D., Ratra, B. 2012, *PLB*, 715, 9  
 Masters, D., et al. 2014, *ApJ*, 785, 153  
 Melnick, J., 1979, *ApJ*, 228, 112  
 Melnick, J., Moles, M., Terlevich, R., & Garcia-Pelayo, J.-M. 1987, *MNRAS*, 226, 849  
 Melnick, J., Terlevich, R., & Moles, M. 1988, *MNRAS*, 235, 297  
 Melnick, J., Terlevich, R., & Terlevich, E., 2000, *MNRAS*, 311, 629  
 Melia, F. 2007, *MNRAS*, 382, 1917  
 Melia, F. 2013, *A&A*, 553, A76  
 Pan, Y., et al. 2015, *ApJ*, 808, 78  
 Perlmutter, S., et al. 1999, *ApJ*, 517, 565  
 Pettini, M., et al. 1998, *ApJ*, 508, 539  
 Planck Collaboration, arXiv:1807.06209  
 Plionis, M., et al. 2011, *MNRAS*, 416, 2981  
 Qi, J.-Z., et al. 2018, *RAA*, 18, 66  
 Qi, J.-Z., et al. 2019, *MNRAS*, 483, 1104  
 Qi, J. Z., et al. 2019, *PRD*, 99, 063507  
 Qi, J. Z., et al. 2019, *PDU*, 26, 100338  
 Riess, A. G., et al., 1998, *ApJ*, 116, 1009  
 Sathyaprakash, B., et al. 2010, *CQG*, 27, 215006  
 Schutz, B. F. *Nature*, 323, 310 (1986).  
 Searle, L., & Sargent, W. L. W. 1972, *ApJ*, 173, 25  
 Seikel, M., Clarkson, C., & Smith, M., 2012, *JCAP*, 6, 036  
 Seikel, M., Yahya, S., Maartens, R., & Clarkson, C., 2012, *PRD*, 86, 083001  
 Siegel, E. R., et al. 2005, *MNRAS*, 356, 1117  
 Taylor, S. R., et al. 2012, *PRD*, 85, 023535  
 Telles, E. 2003, *ASPC*, 297, 143  
 Terlevich, R., et al. 2015, *MNRAS*, 451, 3001  
 Terlevich, R., & Melnick, J. 1981, *MNRAS*, 195, 839  
 The Einstein Telescope Project, <https://www.et-gw.eu/et/>  
 Wei, J.-J., Wu, X.-F., & Melia, F. 2016, *MNRAS*, 463, 1144  
 Xu, T.-P., et al. 2018, *JCAP*, 06, 042  
 Yang, T., et al. 2015, *PRD*, 91, 123533  
 Zhao, W., Van Den Broeck, C., Baskaran, D., & Li, T. 2011, *PRD*, 83, 023005  
 Zheng, X.-G., et al. 2019, *EPJC*, 79, 637